

# PHONEME-TO-VISEME MAPPING FOR VISUAL SPEECH RECOGNITION

Luca Cappelletta and Naomi Harte

*Department of Electronic and Electrical Engineering, Trinity College Dublin, Dublin, Ireland*

Keywords: AVSR, Viseme, PCA, DCT, Optical flow.

Abstract: Phonemes are the standard modelling unit in HMM-based continuous speech recognition systems. Visemes are the equivalent unit in the visual domain, but there is less agreement on precisely what visemes are, or how many to model on the visual side in audio-visual speech recognition systems. This paper compares the use of 5 viseme maps in a continuous speech recognition task. The focus of the study is visual-only recognition to examine the choice of viseme map. All the maps are based on the phoneme-to-viseme approach, created either using a linguistic method or a data driven method. DCT, PCA and optical flow are used to derive the visual features. The best visual-only recognition on the VidTIMIT database is achieved using a linguistically motivated viseme set. These initial experiments demonstrate that the choice of visual unit requires more careful attention in audio-visual speech recognition system development.

## 1 INTRODUCTION

Many authors have demonstrated that the incorporation of visual information into speech recognition systems can improve robustness, as shown in the review paper of Potamianos et al. (Potamianos et al., 2003). In terms of speech recognition as a pattern recognition task, the most common solution is a Hidden Markov Model (HMM)-based system. Phonemes are the typical model unit for continuous speech. Mel-frequency cepstrum (MFCC) is the typical feature. On the visual side, there is less agreement as to the optimal approach even for the most basic early integration schemes.

While many efforts continue to examine visual feature sets to best describe the mouth area, it is also unclear what the optimal modelling units are in the visual domain for continuous speech. At the highest level, the approach is to use visemes, but only a generic definition is recognized. A viseme is defined as a visually distinguishable unit, the equivalent in the visual domain of the phoneme in the audio domain (Potamianos et al., 2003). However there is no agreement on what a viseme is in practice. The most common approach to deriving visemes is to use a hard link between phonemes and their visual manifestation. This is most likely influenced by considering the baseline HMM system to be audio based. Hence a many-to-one phoneme-to-viseme map can be derived.

Many of these maps are present in literature, and there is no agreement on which is the best one.

In this paper five maps created using different methods are compared. All the maps have a varying number of visemes (from 11 to 15, plus a *silence* viseme). In order to compare the performances of the maps, a HMM recognition system is used. The system is trained using different visual feature sets: PCA; DCT; and optical flow. Since the focus of this work is on the visual element of speech recognition initially, visual-only cues were tested for this paper. No audio cues were used. Ultimately, the overall recognition combining audio and visual cues is of interest. This work uses a basic visual HMM system however, in order to focus the problem on the viseme set without the interactions of integration schemes.

In investigating visemes, it is necessary to use a continuous speech database rather than an isolated word recognition task in order to get visemic coverage in the dataset. The most attractive datasets, in terms of number of speakers and sentences uttered, are AVTIMIT (Hazen et al., 2004) and IBM ViaVoice (Neti et al., 2000). Currently, neither is publicly available, so a smaller dataset was used in this work: VIDTIMIT (Sanderson, 2008).

The paper is structured as follows: an overview of viseme definitions is given first along with details of the five phoneme-to-viseme maps used; The feature extraction techniques are presented; and finally

results of a HMM based recognition system are presented for the feature sets and viseme maps. Parameters for the DCT feature extraction scheme are optimised in the experiments reported in this paper, while those for the other feature sets are taken from previous work by the authors.

## 2 VISEME MAPS

As previously stated, visemes have multiple interpretations in the literature and there is no agreement on a way to define them. Two practical definitions are plausible:

- Visemes can be thought of in terms of *articulatory gestures*, such as lips closing together, jaw movement, teeth exposure, etc.
- Visemes are derived from groups of phonemes having the same visual appearance.

The second definition is the most widely used (Potamianos et al., 2003; Saenko, 2004; Neti et al., 2000; Bozkurt et al., 2007), despite a lack of evidence that it is better than the first definition (Saenko, 2004). Using the second approach, visemes and phonemes are strictly correlated, and visemes can be obtained using a *map* of phonemes to viseme. This map has to be a *many-to-one* map, because many phonemes can not be distinguished using only visual cues. This is the approach used in this work. Within this approach, there are two possible ways to build a map:

1. **Linguistic.** Viseme classes are defined through linguistic knowledge and the *intuition* of which phonemes might appear the same visually.
2. **Data Driven.** Viseme classes are formed performing a *phoneme clustering*, based on features extracted from the region of interest around the mouth.

A data driven method has several advantages. Firstly, since most viseme recognition systems use statistical models trained on data, it might be beneficial to automatically learn natural classes from data. Secondly, it can account for contextual variation and differences between speakers (but only if a large database is available) (Saenko, 2004). This is particularly important because the linguistic-based method is usually performed with canonical phonemes in mind, while recognition is done on continuous speech.

All five maps tested in this work have a relatively low number of visemes (from 11 to 15, plus silence viseme) similar to 14 classes present in the MPEG-4 viseme list (Pandzic and Forchheimer, 2003). In other

Table 1: Jeffers phonemes to viseme map (Jeffers and Barley, 1971). The last viseme, /S is used for silence. The table shows the viseme visibility rank and occurrence rate in spoken English.

Viseme	Visibility Rank	Occurrence [%]	TIMIT Phonemes
/A	1	3.15	/f/ /v/
/B	2	15.49	/er/ /ow/ /r/ /q/ /w/ /uh/ /uw/ /axr/ /ux/
/C	3	5.88	/b/ /p/ /m/ /em/
/D	4	.70	/aw/
/E	5	2.90	/dh/ /th/
/F	6	1.20	/ch/ /jh/ /sh/ /zh/
/G	7	1.81	/oy/ /ao/
/H	8	4.36	/s/ /z/
/I	9	31.46	/aa/ /ae/ /ah/ /ay/ /eh/ /ey/ /ih/ /iy/ /y/ /ao/ /ax-h/ /ax/ /ix/
/J	10	21.10	/d/ /l/ /m/ /t/ /el/ /nx/ /en/ /dx/
/K	11	4.84	/g/ /k/ /ng/ /eng/
/S	-	-	/sil/

maps, the viseme number is much higher, e.g. Goldschen map contains 35 visemes (Goldschen et al., 1994).

In the first map, Jeffers & Barley group 43 phonemes into 11 visemes in the English language (Jeffers and Barley, 1971) for what they describe “as usual viewing conditions”. The map linking phonemes to visemes is shown in Table (1). In this table visemes are labelled using a letter, from /A to /K. To these 11, a *silence* viseme has been added, labelled using /S. The last column is a suggested phoneme to viseme mapping for the TIMIT phoneme set. Two phonemes are not listed in the table: /hh/ and /hv/. No specific viseme is linked to them because, while the speaker is pronouncing /hh/ or /hv/, the lips are already in the position to produce the following phoneme. Therefore /hh/ and /hv/ have been merged with the following viseme. The table shows the viseme visibility rank and occurrence rate in spoken English (Jeffers and Barley, 1971). This map is purely linguistic.

The second map analyzed is proposed by Neti *et al.* (Neti et al., 2000). This map has been created using the IBM ViaVoice database and using a decision tree, in the same fashion as decision trees are used to identify triphones. Thus, this map can be considered a mixture of a linguistic and data driven approach. Neti’s map is composed by 43 phonemes and 12 classes (plus a silence class). Details are shown in Table (2)

Hazen *et al.* (Hazen et al., 2004) use a data driven approach. They perform bottom-up clustering using models created from phonetically labelled visual frames. The map obtained is “roughly” (Hazen et al., 2004) based on this clustering technique. The

Table 2: Neti map (Neti et al., 2000).

Code	Viseme Class	Phonemes in Cluster
V1	Lip-rounding based vowels	/ao/ /ah/ /aa/
V2		/er/ /oy/ /aw/ /hh/
V3		/uw/ /uh/ /ow/
V4		/ae/ /eh/ /ey/ /ay/ /ih/ /iy/ /ax/
A	Alveolar-semivowels	/l/ /el/ /r/ /y/
B	Alveolar-fricatives	/s/ /z/
C	Alveolar	/t/ /d/ /n/ /en/
D	Palato-alveolar	/sh/ /zh/ /ch/ /jh/
E	Bilabial	/p/ /b/ /m/
F	Dental	/th/ /dh/
G	Labio-dental	/f/ /v/
H	Velar	/ng/ /k/ /g/ /w/
S	Silence	/sil/ /sp/

Table 3: Hazen map (Hazen et al., 2004).

Viseme Class	Phonemes Set
OV	/ax/ /ih/ /iy/ /dx/
BV	/ah/ /aa/
FV	/ae/ /eh/ /ay/ /ey/ /hh/
RV	/aw/ /uh/ /uw/ /ow/ /ao/ /w/ /oy/
L	/el/ /l/
R	/er/ /axr/ /r/
Y	/y/
LB	/b/ /p/
LCl	/bcl/ /pcl/ /m/ /em/
AlCl	/s/ /z/ /epi/ /tcl/ /dcl/ /n/ /en/
Pal	/ch/ /jh/ /sh/ /zh/
SB	/t/ /d/ /th/ /dh/ /g/ /k/
LFr	/f/ /v/
VIcI	/gcl/ /kcl/ /ng/
Sil	/sil/

reason for this apparent inaccuracy is that the clustering results vary a lot depending on the visual feature used. Hazen *et al.* group 52 phonemes into 14 visemes (plus a silence viseme). This is shown in Table (3).

Bozkurt *et al.* (Bozkurt et al., 2007) created a map using the linguistic approach. The map is based on Ezzat and Poggio’s work (Ezzat and Poggio, 1998), in which they define the phoneme clustering as “done in a subjective manner, by comparing the viseme images visually to assess their similarity”. The Bozkurt map comprises 15 viseme (plus a silence viseme), and 45 phonemes detailed in Table (4).

In the final map shown in Table (5), Lee and Yook (Lee and Yook, 2002) identify 13 (plus a silence viseme) viseme classes from 39 phonemes (plus a silence phoneme and a pause phoneme). They do not explain how the map has been derived, so it has

Table 4: Bozkurt Map (Bozkurt et al., 2007).

Viseme Class	Phonemes Set
S	sil
V2	ay, ah
V3	ey, eh, ae
V4	er
V5	ix, iy, ih, ax, axr,y
V6	uw, uh, w
V7	ao, aa, oy, ow
V8	aw
V9	g, hh, k, ng
V10	r
V11	l, d, n, en, el, t
V12	s, z
V13	ch, sh, jh, zh
V14	th, dh
V15	f, v
V16	m, em, b, p

Table 5: Lee Map (Lee and Yook, 2002).

Viseme Class	Phonemes Set
P	b p m
T	d t s z th dh
K	g k n ng l y hh
CH	jh ch sh zh
F	f v
W	r w
IY	iy ih
EH	eh ey ae
AA	aa aw ay ah
AH	ah
AO	ao oy ow
UH	uh uw
ER	er
S	sil

been assumed it is a linguistic map. Even though they claim this is a many-to-one map, some phonemes are mapped into 2 visemes, so the map is a many-to-many map. To remove this ambiguity, in such cases phonemes are associated with the first viseme proposed. This affects 5 vowel phonemes.

It is not a simple task to compare these maps because the total viseme number and the total phoneme number are different in the five maps. Table 6 sums up the most relevant map properties. It is clear that some similarities are present, particularly between the Jeffers and Neti maps. In these two maps 5 consonant classes are identical. Across all maps, the consonant classes show similar class separation. All the maps have a specific class for phoneme clusters {v/, /f/} and {/ch/, /jh/, /sh/, /zh/}. Jeffers, Neti,

Table 6: Map properties. Clustered phoneme number, number of visemes and number of vowel visemes. Silence viseme and phonemes are not taken into consideration.

Map	Phonemes	Total Visemes	Vowel Visemes
Jeffers	43	11	4
Neti	42	12	4
Hazen	52	14	5
Bozkurt	45	15	7
Lee	39	13	7

Bozkurt and Lee have a specific class for  $\{/b/, /m/ /p/\}$ . Group  $\{/th/, /dh/\}$  forms a viseme in Jeffers, Neti and Bozkurt, while in Hazen and Lee it is merged with other phonemes. Aside from this, the Hazen map (the only data driven map) is significantly different from the others, while Jeffers and Neti have an impressive consonant class correspondence.

In contrast, vowel visemes are quite different from map to map. The number of vowel visemes varies from 4 to 7, and a single class can contain from 1 up to 10 vowels. No specific cross-map patterns are present within maps.

A final difference within the maps is that the phonemes  $\{/pcl/, /tcl/, /kcl/, /bcl/, /dcl/, /gcl/, /epi/\}$  are not considered in the analysis by Jeffers, Neti, Bozkurt and Lee, while they are spread across several classes by Hazen.

### 3 FEATURE EXTRACTION

Feature extraction is performed in two consecutive stages, a *Region of Interest* (or ROI) has to be detected and then a feature extraction technique is applied to the area. The ROI is found using a semi-automatic technique (Cappelletta and Harte, 2010) based on two stages: the speaker’s nostrils are tracked and then, using those positions, the mouth is detected. The first stage succeeds on the 74% of the database sentences, so the remaining 26% has been manually tracked to allow experimentation on the full dataset. The second stage has 100% success rate. Subsequently the ROI is rotated according to the nostrils alignment. At this stage the ROI is a rectangle, but its size might vary in each frame. Thus, ROIs are either stretched or squeezed until they have the same size. The final size is the mode calculated using all ROIs size.

Having defined the region of interest, a feature extraction algorithm is applied to the ROI. Three different appearance-based techniques were used: Optical Flow; PCA (principal component analysis); and DCT (discrete cosine transform).

Optical flow is the distribution of apparent veloci-

ties of movement of brightness pattern in an image. The code used in (Bouquet, 2002) implements the Lucas-Kanade technique (Lucas and Kanade, 1981). The output of this algorithm is a two dimensional speed vector for each ROI point. A data reduction stage, or *downsampling*, is required. The ROI is divided in  $d_R \times d_C$  blocks, and for each block the median of the horizontal and vertical speed is calculated. In this way  $d_R \cdot d_C$  2D speed vectors are obtained.

PCA (also known as *eigenlips* in AVSR applications (Bregler and Konig, 1994)) and DCT are similar techniques. They both try to represent a video frame using a set of coefficients obtained by the image projection over an orthogonal base. While the DCT base is a priori defined, the PCA base depends on the data used. The optimal number of coefficients  $N$  (the feature vector length) is a key parameter in the HMM creation and training. A vector too short would lead to a low quality image reconstruction, too long a feature vector would be difficult to model with a HMM. DCT coefficients are extracted using the zigzag pattern and the first coefficient is not used.

Along with these features, first and second derivatives are used, defined as follows:

$$\begin{aligned} \Delta_k[i] &= F_k[i+1] - F_k[i-1] \\ \Delta\Delta_k[i] &= \Delta_k[i+1] - \Delta_k[i-1] \end{aligned} \quad (1)$$

where  $i$  represents the frame number in the video, and  $k \in [1..N]$  represents the  $k$ th generic feature  $F$  value. Used with PCA and DCT coefficients,  $\Delta$  and  $\Delta\Delta$  represent speed and acceleration in feature evolution. Both  $\Delta$  and  $\Delta\Delta$  have been added to PCA and DCT features. While optical flow already represents ROI elements speed, only  $\Delta$  has been tested with it.

Optimal optical flow and PCA parameters have already been investigated and reported by the authors for this particular dataset (Cappelletta and Harte, 2011). Results showed that an increment of PCA vector length does not improve the recognition rate figure with an optimal value of  $N = 15$ . The best performance is obtained using  $\Delta$  and  $\Delta\Delta$  coefficients, without the original PCA data. Similarly, the best performance with optical flow was achieved using original features with  $\Delta$  coefficients. In this case performance is not affected by different downsampling configurations. Thus, the  $2 \times 4 + \Delta$  configuration will be used for experiments reported in this paper.

## 4 EXPERIMENT

### 4.1 VIDTIMIT Dataset

The VIDTIMIT dataset (Sanderson, 2008) is com-

prised of the video and corresponding audio recordings of 43 people (24 male and 19 female), reciting 10 short sentences each. The sentences were chosen from the test section of the TIMIT corpus. The selection of sentences in VIDTIMIT has full viseme coverage for all the maps used in this paper. The recording was done in an office environment using a broadcast quality digital video camera at 25 fps. The video of each person is stored as a numbered sequence of JPEG images with a resolution of 512 x 384 pixels. 90% quality setting was used during the creation of the JPEG images. For the results presented in this paper, 410 videos have been used and they have been split in a *training* group (297 sentences) and a *test* group (113 sentences). The two groups are balanced in gender and they have similar phoneme occurrence rates. Training and test speakers did not overlap.

## 4.2 HMM Systems

HMMs were trained using PCA, DCT and optical flow features. A visemic time transcription for VIDTIMIT was generated using a forced alignment procedure with monophone HMMs trained on the TIMIT audio database. The system was implemented using HTK. All visemes were modelled with a left-to-right HMM, except silence which used a fully ergodic model. The number of mixtures per state was gradually increased, with Viterbi recognition performed after each increase to monitor system performance. No language model was used in order to assess raw feature performance. The feature vector rate was increased to 20ms using interpolation. Both a 3 and 4-state HMM were used.

The experiment was conducted in two stages. In the first stage the Jeffers map was used. The HMM and DCT feature parameters were varied in order to find the optimal parameter configuration. It should be noted that similar results were achieved using the other maps but space limits the presentation of these results to a single map. In particular, the recognition rate is tested varying the HMM mixture number. Results are compared with PCA and optical flow feature performance.

In the second stage of the experiments, the feature set parameters were fixed (using the optimal configurations in (Cappelletta and Harte, 2011) and those determined for the DCT), in order to compare the results from different maps. The optimal number of mixtures for each individual viseme class was tracked. This overcomes issues with different amounts of training data in different classes. Thus HMMs used between 1 and 60 mixtures per state.

## 5 RESULTS

### 5.1 Feature Set Parameters

HMM results are assessed using the *correctness* estimator, *corr*, defined as follows:

$$Corr = \frac{T - D - S}{T} \times 100 \quad (2)$$

where T is the total number of labels in the reference transcriptions, D is the deletion error and S is the substitution error.

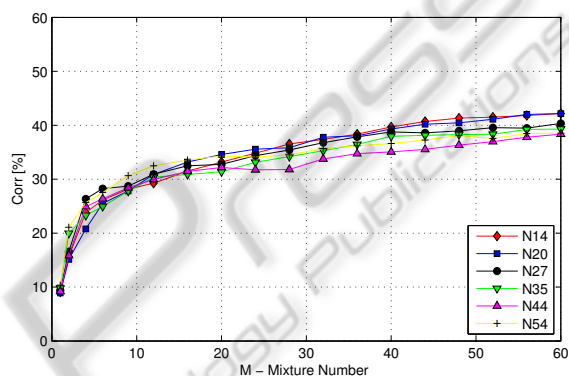


Figure 1: Basic DCT test, 3 States. N14, N20 refer to number of DCT features at 14, 20 etc..

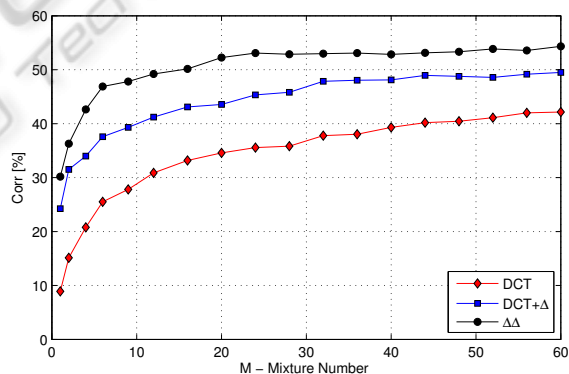


Figure 2: Higher order DCT features.  $N = 20$ , 3 States. DCT denotes 20 DCT features only, DCT+ $\Delta$  denotes addition of first order dynamics,  $\Delta\Delta$  denotes inclusions of both first and second order dynamics without original DCT coefficients.

Figures 1 and 2 show the correctness of the 3-state HMM using DCT features and the Jeffers map. Results for the 4-state HMM are not shown because no significant improvement from the 3-state was achieved. Figure 1 shows the results of the basic DCT coefficient tests obtained by varying the feature vector length  $N$  between 14 and 54. The best results are achieved with a vector length of 14 and 20, even though all the configurations achieve very similar results, according to

Heckmann *et al.* (Heckmann et al., 2002). Significant improvement can be achieved using  $\Delta$  and  $\Delta\Delta$ . Figure 2 shows the performance of 20 DCT coefficients with first and second derivatives added. The recognition rate is increased by at least 30%. This behaviour mirrors that of the PCA feature set. As might be expected, no significant improvement is achieved behind 35 Gaussian mixtures.

## 5.2 Maps Comparison

In the second part of the experiment, all the maps were tested. The PCA and DCT results are obtained using  $\Delta$  and  $\Delta\Delta$  coefficients only, using  $N = 15$  for PCA, and  $N = 20$  for the DCT feature set. Optical flow results are obtained using  $2 \times 4$  downsampling with  $\Delta$  coefficients. Along with correctness, defined in equation 2, it is advisable to use the *accuracy* estimator to give a better overall indication of performance. The standard definition was used:

$$Acc = \frac{T - D - S - I}{T} \times 100 \quad (3)$$

where  $I$  is the number of insertions.

Figure 3 and Figure 4 show recognition results for the five maps. When examining the figures, it is important to realise that recognition results in a continuous speech task are expected to be relatively low when compared to, for example, an isolated digit task. It can certainly be argued that results will improve significantly with use of a language model and when combined with audio cues. However, this viseme set exploration is seeking to study baseline viseme performance initially.

It is apparent that the Jeffers map gives the best results both in terms of correctness and accuracy. The Neti map is the next best map, with little difference in performance from the remaining maps. Examining the *accuracy* figures, it is clear that the insertion level remains high overall. An insertion penalty was investigated in an attempt to address this issue but a suitable balance has not yet been found for the system. The performance for the optical flow and PCA features using 3-state HMMs was little better than a guess rate.

It is possible to see a correlation between recognition rate and the number of viseme and vowel classes listed in Table 6. The lower the viseme and vowel class number, the better the recognition figure. Whilst this is fully expected in a pattern recognition task, it is still interesting to compare the Jeffers and Neti maps because, even though many visemes encompass the same phonemes (5 classes are identical), the results are quite different. Results from 3-states HMM with optical flow feature are used to demonstrate this, but

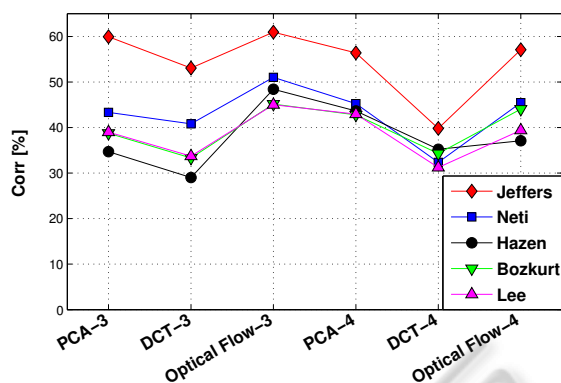


Figure 3: 3- and 4-states HMM correctness for each map, using all feature extraction techniques. Jeffers map gets the best performance in all tests, considering both 3- and 4-states.

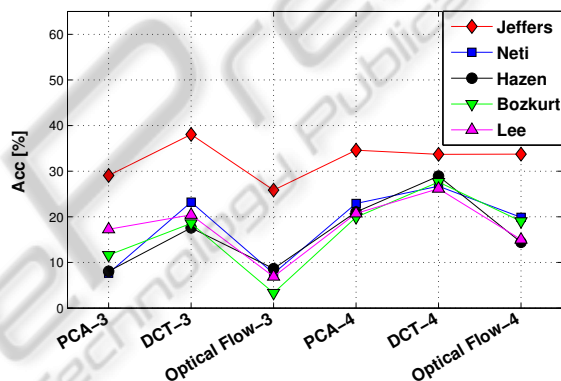


Figure 4: 3- and 4-states HMM accuracy for each map, using all feature extraction techniques. While Jeffers map still gets good results, some maps reach the guessing rate level (different for each map, see Table 6).

other feature sets yield similar conclusions. Figure 5 and Figure 6 show the confusion matrices obtained using 3-states HMM optical flow tests. Total label number, deletion number and substitution number are also provided (see equation 2).

As expected the 5 identical classes ( $/H \equiv B$ ,  $/F \equiv D$ ,  $/C \equiv E$ ,  $/E \equiv F$  and  $/A \equiv G$ ) obtain basically the same results. Thus, the Neti performance gap has to be in the remaining consonant classes and in the vowel visemes. Considering the vowel classes, it is possible to see that in terms of number of phonemes covered, Jeffers has two big ( $/B$  and  $/I$ ) and two very small ( $/D$  and  $/G$ ) vowel classes. In contrast, Neti has four quite balanced vowel classes ( $V1-V4$  contain almost the same number of phonemes). Jeffers has an advantage because misclassification is less probable if classes are big (see  $/B$  and  $/I$  in Figure 5). Moreover, even a complete misclassification in the two small classes will have a minor impact on the overall recognition

/A	11	12	8	1	1	4		2	10	28	2	3	25	71
/B	4	286	13	3	5	7		3	27	67		15	66	144
/C	2	13	110	3	4	1		4	8	26		13	41	74
/D		2		1				1	4	1		1	1	9
/E	1	11	7	1	9	2			7	22	1	4	13	56
/F		18	6	2	2	16		1	11	17	2	6	19	65
/G		3		2		3		1	4	2	1	1	7	17
/H	1	35	8	4	1	6	1	37	25	67		19	61	167
/I	1	29	7	4	1	2	1	2	887	49		22	73	118
/J	5	19	17		3	6		3	15	547	1	14	48	83
/K	5	19	11	2	2	12		8	27	51	18	14	66	151
/S												226	0	0
	/A	/B	/C	/D	/E	/F	/G	/H	/I	/J	/K	/S	del	sub

Figure 5: Confusion matrix obtained with 3-states HMM using optical flow feature and Jeffers map. /B, /D, /G and /I are the vowel visemes. Sub column represents the substitution error for each viseme, while del represents the deletion error for each viseme.  $T = 3523, D = 420, S = 955$  (see eq. 2).

rate. Figure 5 shows that /D and /G are basically completely misclassified, mostly in favour of the other two vowel classes /B and /I, but these classes have such a low occurrence that this misclassification is negligible from a statistical point of view. On the contrary, Neti vowel visemes are more frequently misclassified. They contribute roughly 60% more classification error, either in substitution or deletion errors.

Similar behaviour is present in the remaining consonant classes. The remaining consonant phonemes are clustered in two visemes in Jeffers map (/K and /J) and in three visemes in Neti map (A, H and C). Once again, the lesser the class number, the better the classification. The three Neti visemes contribute 40% more error than the two Jeffers consonant visemes.

## 6 CONCLUSIONS AND FUTURE WORK

This paper has presented a continuous speech recognition system based purely on HMM modelling of visemes. A continuous recognition task is significantly more challenging than isolated word recognition task such as digits. In terms of AVSR, it is a more complete test of a system's ability to capture pertinent information from a visual stream, as the complete set of visemes is present in a greater range of contexts. Five viseme maps have been tested, all based on the phonemes-to-viseme map technique. These maps were created using different approaches (linguistic, data driven and mixed). A pure linguistic map (Jef-

A	238	6	35	5	7	9	1	9	11	7	17	13	17	57	137
B	22	51	50	4	6	1	2	15	12	9	10	14	10	59	155
C	23	4	390	2	4	4	3	8	15	3	10	8	8	34	92
D	14	2	11	17		4		12	4	6	1	4	3	22	61
E	17	4	20		101	2	2	7	9	1	12	10	6	34	90
F	10	1	15	1	2	9		5	4	2	1	2	6	20	49
G	8	5	12	1	5	1	12	6	2	4	6	7	8	30	65
H	10	6	32	2	5	1	5	130	7	4	13	16	9	65	110
V1	16	3	24	2	2	2		8	266	21	32	30	26	81	166
V2	10	2	13	3	3		1	5	11	49	6	6	10	38	70
V3	20	7	18		5	2		4	15	12	175	17	16	37	116
V4	17	3	38	3	1	6	2	8	23	10	24	205	16	54	151
S												226	0	0	0
	A	B	C	D	E	F	G	H	V1	V2	V3	V4	S	del	sub

Figure 6: Confusion matrix obtained with 3-states HMM using optical flow feature and Neti map. V1 to V4 are the vowel visemes. Sub column represents the substitution error for each viseme, while del represents the deletion error for each viseme.  $T = 3662, D = 531, S = 1262$  (see eq. 2).

fers) achieved the best recognition rates in all the performed tests. Compared with the second best map (Neti), this improvement in performance can be attributed to better clustering in some consonant classes and less vowel visemes (statistically, Jeffers visemes /D and /G are negligible).

Work is ongoing to extend this system to include other feature sets including other optical flow implementations and *Active Appearance Model* (AMM) features to provide a definitive baseline for visual speech recognition. To validate whether the Jeffers map is a better approach to viseme modeling in the context of a full AVSR system, the maps are also being tested incorporating speech features. This will test the hypothesis that better visual features should improve the overall AVSR performance when the speech quality is low.

Unfortunately, the phonemes-to-viseme map approach does not take into account audio-visual asynchrony (Potamianos et al., 2003; Hazen, 2006), nor the fact that some phonemes do not require the use of visual articulators, such /k/ and /g/ (Hilder et al., 2010). Thus, along with the tested maps, it is important to include in the analysis viseme definitions that do not assume a formal link between acoustic and visual speech cues. This will emphasize the dynamics in human mouth movements, rather than the audio-visual link only.

To this end, the availability of large continuous speech AVSR datasets (as opposed to isolated word tasks or databases containing a small number of sentences), continues to be a hurdle in AVSR development.

## ACKNOWLEDGEMENTS

This publication has emanated from research conducted with the financial support of Science Foundation Ireland under Grant Number 09/RFP/ECE2196.

## REFERENCES

- Bouquet (2002). Pyramidal Implementation of Lucas Kanade Feature Tracker. Description of the algorithm.
- Bozkurt, Eroglu, Q., Erzin, Erdem, and Ozkan (2007). Comparison of phoneme and viseme based acoustic units for speech driven realistic lip animation. In *3DTV Conference, 2007*, pages 1–4.
- Bregler and Konig (1994). ‘Eigenlips’ for robust speech recognition. In *Acoustics, Speech, and Signal Processing, 1994. ICASSP-94., 1994 IEEE International Conference on*, volume ii, pages II/669–II/672 vol.2.
- Cappelletta and Harte (2010). Nostril detection for robust mouth tracking. In *Irish Signals and Systems Conference*, pages 239 – 244, Cork.
- Cappelletta, L. and Harte, N. (2011). Viseme definitions comparison for visual-only speech recognition. In *Proceedings of 19th European Signal Processing Conference (EUSIPCO)*, pages 2109–2113.
- Ezzat and Poggio (1998). Miketalk: a talking facial display based on morphing visemes. In *Computer Animation 98. Proceedings*, pages 96–102.
- Goldschen, A. J., Garcia, O. N., and Petajan, E. (1994). Continuous optical automatic speech recognition by lipreading. In *Proceedings of the 28th Asilomar Conference on Signals, Systems, and Computers*, pages 572–577.
- Hazen (2006). Visual model structures and synchrony constraints for audio-visual speech recognition. *Audio, Speech, and Language Processing, IEEE Transactions on*, 14(3):1082–1089.
- Hazen, Saenko, La, and Glass (2004). A segment-based audio-visual speech recognizer: data collection, development, and initial experiments. In *Proceedings of the 6th international conference on Multimodal interfaces*, pages 235–242, State College, PA, USA. ACM.
- Heckmann, Kroschel, Savariaux, and Berthommier (2002). DCT-Based Video Features for Audio-Visual Speech Recognition. In *International Conference on Spoken Language Processing*, volume 1, pages 1925–1928, Denver, CO, USA.
- Hilder, Theobald, and Harvey (2010). In pursuit of visemes. In *International Conference on Auditory-visual Speech Processing*.
- Jeffers and Barley (1971). *Speechreading (Lipreading)*. Charles C Thomas Pub Ltd.
- Lee and Yook (2002). Audio-to-Visual Conversion Using Hidden Markov Models. In *Proceedings of the 7th Pacific Rim International Conference on Artificial Intelligence: Trends in Artificial Intelligence*, pages 563–570. Springer-Verlag.
- Lucas and Kanade (1981). An iterative image registration technique with an application to stereo vision. In *Proceedings of Imaging Understanding Workshop*.
- Neti, Potamianos, Luetin, Matthews, Glotin, Vergyri, Sison, Mashari, and Zhou (2000). Audio-visual speech recognition. Technical report, Center for Language and Speech Processing, The Johns Hopkins University, Baltimore.
- Pandzic, I. S. and Forchheimer, R. (2003). *MPEG-4 Facial Animation: The Standard, Implementation and Applications*. John Wiley & Sons, Inc., New York, NY, USA.
- Potamianos, Neti, Gravier, Garg, and Senior (2003). Recent advances in the automatic recognition of audio-visual speech. *Proceeding of the IEEE*, 91(9):1306–1326.
- Saenko, K. (2004). *Articulatory Features for Robust Visual Speech Recognition*. Master thesis, Massachusetts Institute of Technology.
- Sanderson (2008). *Biometric Person Recognition: Face, Speech and Fusion*. VDM-Verlag.